Brain Pathology ISSN 1015-6305

RESEARCH ARTICLE: Molecular Changes in MS Periplaque White Matter

Molecular Changes in White Matter Adjacent to an Active Demyelinating Lesion in Early Multiple Sclerosis

Thomas Zeis[1]; Alfonse Probst[2]; Andreas Johann Steck[1]; Christine Stadelmann[3]; Wolfgang Brück[3]; Nicole Schaeren-Wiemers[1]

[1] Neurobiology, Department of Biomedicine and Neurology, University Hospital Basel, Pharmacenter, Basel, Switzerland.
[2] Institute of Neuropathology, University Hospital Basel, Basel, Switzerland.
[3] Institute of Neuropathology, Georg-August-University Göttingen, Göttingen, Germany.

Keywords
multiple sclerosis, oligodendrocyte pathology, oxidative stress, white matter injury.

Corresponding author:
Nicole Schaeren-Wiemers, PhD, Neurobiology, Department of Biomedicine and Neurology, University Hospital Basel, Pharmacenter 7007, Klingelbergstrasse 50/70, Basel CH-4056, Switzerland (E-mail: *Nicole.Schaeren-Wiemers@unibas.ch*)

Received 14 August 2008; accepted 10 September 2008.

doi:10.1111/j.1750-3639.2008.00231.x

Abstract

A stereotactic biopsy of a 17-year-old woman revealed an active inflammatory demyelinating lesion compatible with pattern III multiple sclerosis (MS) according to Lucchinetti *et al*. The biopsy included a white matter region distant from the active inflammatory demyelinating lesion with abnormal MRI signal, lacking histopathological signs of demyelination and/or oligodendrocyte apoptosis. Expression analysis of this area revealed a strong up-regulation of neuronal nitric oxide synthase (nNOS). Furthermore, detection of nitrotyrosine provided evidence for reactive nitrogen species (RNS)-mediated damage to oligodendrocytes. Concomitantly, genes involved in neuroprotection against oxidative stress such as heme oxygenase 1 were up-regulated. Even though a single case report, this study shows earliest molecular changes in white matter surrounding an actively demyelinating lesion during the first manifestation of MS, pointing toward a more widespread pathological process. Therapeutic targeting of the identified mechanisms of tissue injury might be crucial to prevent further lesion formation or secondary tissue damage.

Abbreviations: AQP4, aquaporin 4; CNS, central nervous system; EGR1/Krox20, early growth response protein 1; GFAP, glial fibrillary acid protein; HIF1α, hypoxia-inducible transcription factor 1alpha; HLA-DRA, major histocompatibility complex alpha-chain; HO-1/HSP32, heme oxygenase 1/heat shock protein 32; HSP70.1, heat shock protein 70.1; MAG, myelin-associated glycoprotein; MOG, myelin oligodendrocyte glycoprotein; MRI, magnetic resonance imaging; MS, multiple sclerosis; NAWM, normal appearing white matter; NO, nitric oxide; NOS, nitric oxide synthase; eNOS, endothelial isoform of NOS; iNOS, inducible isoform of NOS; nNOS, neuronal isoform of NOS; PDGFRα, platelet-derived growth factor receptor alpha; PLP, proteolipid protein; RNS, reactive nitrogen species; qRT-PCR, quantitative reverse transcriptase polymerase chain reaction; STAT, signal transducers and activators of transcription; TAUT, taurine transporter; TUNEL, terminal deoxynucleotidyl transferase-mediated dUTP-nick end labeling; VEGFR, vascular endothelial growth factor receptor

INTRODUCTION

MS is a chronic, inflammatory, demyelinating disease of the CNS with great heterogeneity in clinical course, response to therapy, and lesion pathogenesis. In 2000, four different patterns of demyelination were suggested (14). One of these, pattern III, is characterized by an early selective loss of MAG associated with oligodendrocyte apoptosis. Oligodendrocyte apoptosis in the absence of significant inflammatory cell infiltrates has also been described as a possible initial event of lesion formation, and has been designated as "pre-phagocytic" stage of demyelinating MS lesions (1). As a potential cause of oligodendrocyte apoptosis in MS, NO was suggested (25). Recently, one isoform of NOS, nNOS, was reported to play a key role in CNS demyelination (13). In our study, we analyzed white matter from a patient with early MS, without signs of demyelination or oligodendrocyte apoptosis (from a region with abnormal T1 and T2 weighted MRI signal) in vicinity to an actively demyelinating pattern III lesion. Gene expression analysis revealed strong up-regulation of nNOS, but only minor up-regulation of iNOS and eNOS. This and the finding of nitrotyrosine-immunoreactive oligodendrocytes, indicative of NO-mediated damage, support the view of global damage to the brain, especially oligodendrocytes, in the earliest disease stages of MS. These changes may represent early molecular events preceding demyelination or pathogenetically relevant secondary tissue reactions. Although this is a single case study, and therefore, interindividual gene expression variation

could not be evaluated, our study demonstrates widespread molecular changes in the MS brain in an early disease stage, and may thus add important knowledge for further understanding of MS pathogenesis.

METHODS

Stereotactic brain biopsy and histopathological examination

Biopsy specimens were taken from a 17-year-old woman (Table 1) from three different target regions in the frontal subcortical white matter (Figure 1B,D). Four biopsy specimens were formalin fixed and embedded in paraffin (three) or epon (one) for diagnostic purposes; two others were snap frozen for RNA extraction and transferred to our lab for molecular analysis. Conventional myelin staining was performed with Holmes/Luxol. Immunohistochemical staining was performed as described before (10, 15, 27). Detection of RNS, in particular peroxynitrite-mediated damage was performed by immunofluorescent staining with anti-nitrotyrosine antibody as described before (11). For detection of fragmented DNA, TUNEL was used as described before (26).

Autopsy tissue

MS and control autopsy tissue samples (Table 1) were kindly supplied by the UK Multiple Sclerosis Tissue Bank (UK Multicentre Research Ethics Committee, MREC/02/2/39), funded by the Multiple Sclerosis Society of Great Britain and Northern Ireland (registered charity 207495), and previously used for microarray studies (10, 30). All tissues have been screened by a neuropathologist to confirm diagnosis of MS and to exclude other confounding pathologies. Bielschowsky silver stain and β-amyloid immunostaining screening revealed a small number of diffuse amyloid plaques in the entorhinal cortex in a number of the cases, but no pathological changes could be seen. Nevertheless, additional age-related pathologies influencing gene expression patterns cannot be excluded completely.

Control biopsy tissue

Control biopsy tissues (Table 1) was supplied by the Department of Neuropathology, University Medical Centre Göttingen from two stereotactic brain biopsies of a 10-year-old female (CBps1) and a 43-year-old male (CBps2). From both patients, several tissue specimens were taken stereotactically that reached from the normal white matter to the tumor (malignant glioma in both cases). The white matter specimens of both cases did not show any signs of glioma (increased cellularity, pleomorphism, mitoses) or tumor cell infiltration, whereas a slight astrocytic gliosis was present. These two specimens were used for RNA isolation.

RNA isolation and quantitative RT-PCR analysis

Total RNA isolation and quantitative RT-PCR analysis of all samples were performed as previously described (10, 30). Normalization of calculated RNA amounts by qRT-PCR was done by using 60 s ribosomal protein L13 (NM_031101.1). Fold changes were calculated by comparison of the normalized raw data from the biopsy to the control autopsies. Expression data obtained from the biopsy of the patient were compared to expression levels of the subcortical white matter from brain tissue obtained from postmortem (p.m.) control cases and NAWM of MS cases. In addition, expression data were also compared to two disease control

Table 1. Patient data.

	Patient ID	Age (year)	Sex	Cause of death
p.m. control cases	CLo7	77	M	Lung cancer
	CLo8	64	F	Cardiac failure
	CLo9	36	M	Carcinoma of the tongue
	CBS1	70	M	Myocardial infarction
	CBS2	66	M	Bronchocarcinoma
	CBS4	69	M	Myocardial infarction
	CBS5	59	F	Acute pancreatitis
p.m. MS cases	MS1	56	F	Bilater basal pneumonia
	MS2	58	F	Peritonitis
	MS3	76	F	Myocardial infarction
	MS5	58	F	Bronchopneumonia
	MS10	69	F	Acute pyelonephritis
	MS12	78	F	Lung infection
	MS18	78	F	Bronchocarcinoma
	MS25	54	F	Bronchopneumonia
	Patient ID	Age (year)	Sex	Diagnosis of
Control biopsy tissue	CBps1	10	F	Malignant glioma
	CBps2	43	M	Malignant glioma
Index patient	Bps1	17	F	Multiple sclerosis

Patient data of MS and control cases. Clinical and pathological information concerning the 7 p.m. control cases, the 8 p.m. MS cases, the two control biopsy cases as well as the index patient is shown. All samples were used for the qRT-PCR analysis.

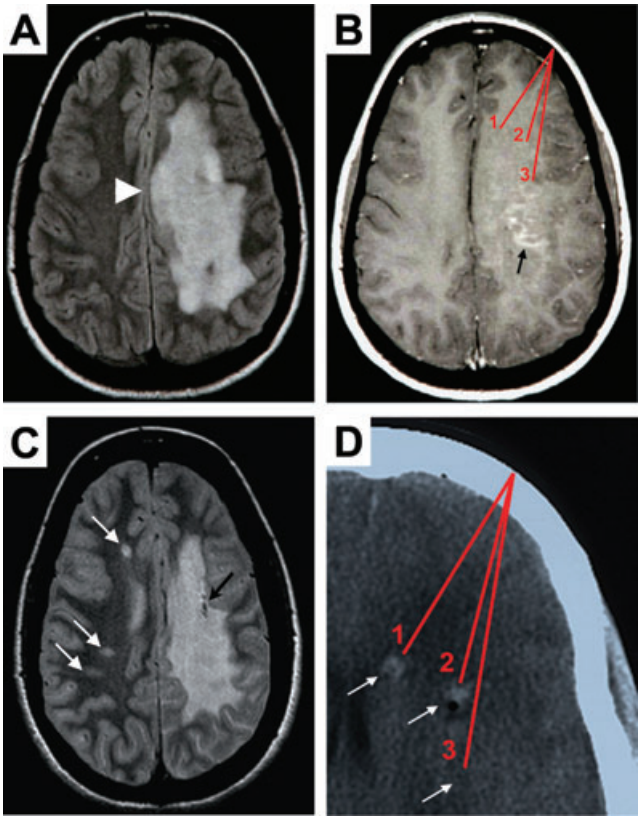

Figure 1. *MRI analysis of the index patient.* A T2-weighted MRI during the first manifestation displays a large confluent hyperintense lesion in the subcortical white matter of left hemisphere (**A**) with mass effect (arrowhead). Gadolinium-enhanced T1-weighted MRI revealed a punctate, garland-like enhancement in the subcortical white matter (**B**, arrow). Red lines mark schematically the three target regions from which the stereotactic biopsy specimens were taken (**B**). A routine follow-up MRI investigation after 5 years revealed three new white matter lesions in the contralateral hemisphere (**C**, white arrows). Black arrow points to tissue destruction by one of the stereotactic brain biopsies (**C**). A CT picture (**D**) illustrates the three target regions (1, 2, 3) of the biopsy specimens taken from the frontal subcortical white matter (arrows). Note, CT signal enhancement by bleedings caused by the excision of tissue is visible (**D**, arrows 1 and 2). Note that the origin of all biopsy specimens was in regions of abnormal T1, T2, and CT signals, but only some biopsy specimens contained inflammatory demyelinating lesion, whereas others contained histomorphologically normal appearing white matter only.

biopsies, CBps1 and CBps2. As the amount of RNA derived from the index patient was very limited, qRT-PCR analysis was performed at least in duplicates and for particular genes (e.g. nNOS, iNOS) in triplicates.

RESULTS

Case report

A previously healthy, 17-year-old woman was hospitalized with subacute progressive global aphasia, right-sided hemiparesis, difficulty in walking, and dysphagia. Neurological examination revealed right-sided hemianopsia and right hemiplegia with hemihypaesthesia with extensor plantar response. Laboratory tests for rheumatic factors, antinuclear antibodies, c-ANCA, p-ANCA, as well as CNS serology for HIV, HSV, VSZ, measles, mumps, FSME, syphilis, and Lyme disease were negative. Urine sediment, as well as vitamins B12, B1, and E were normal. Analysis of the cerebrospinal fluid revealed a pleocytosis (43 leukocytes $\times 10^6$/L; normal value <5), increased protein (548 mg/L; normal value 180–480 mg/L), and more than five oligoclonal bands. T1-weighted MRI showed a large hypointense lesion of the subcortical white matter extending throughout the left hemisphere, hyperintense on T2-weighted scans (Figure 1A). Gadolinium-enhanced T1 MRI revealed a punctate garland-like enhancement in the fronto-parietal subcortical white matter (Figure 1B, arrow), which was only seen on the second MRI, 10 days after admission. Because of the pseudotumoral lesion characteristics, stereotactic biopsy from three different target regions in the frontal subcortical white matter was undertaken on day 15 of hospitalization (Figure 1B,D). Initial high-dose steroid treatment followed by a course of i.v. immunoglobulins did not lead to a therapeutic response, whereas in subsequent months there was a slow improvement of the neurological deficits. No relapses occurred in the following 5 years. In a routine follow-up MRI investigation 5 years after the initial presentation, two new lesions were observed in the contralateral hemisphere (Figure 1C, arrows). Two months later, a relapse occurred with increased ataxia, aphasia, and sensory motor impairment on the right side. Brain MRI displayed new lesions with diffusion restriction and gadolinium enhancement in the left brachium pontis (not shown). The patient underwent steroid and mitoxantrone therapy. After further 5 months, she suffered from another relapse with hyperaesthesia of the left leg. Spinal MRI showed intramedullar hyperintense lesions in the cervical (C2) and thoracic (Th5/6 and Th10/11) spinal cord. Thus, she fulfilled the diagnostic criteria for MS (16, 17).

The active demyelinating lesion reveals MS pattern III-like pathology

In one of the three formalin-fixed and paraffin-embedded biopsy specimens taken from target region 1 (Figure 1B,D), a demyelinating lesion was seen (Figure 2A) with perivascular lymphocytic cuffs (Figure 2A, inset arrow) and dense infiltrates of foamy macrophages (Figure 2B) containing MOG-positive myelin debris (Figure 2E, arrows) indicating early active demyelination. In contrast to MOG and PLP (Figure 2C), the specific absence of MAG (Figure 2D) was apparent. In addition, oligodendrocytes with dark and fragmented nuclei suggestive of apoptosis were found within the lesion, which was confirmed by TUNEL staining (Figure 2F, arrow). Altogether, this pathology is in agreement with a pattern III lesion type according to Lucchinetti *et al* 2000 (14).

White matter with no signs of demyelination or inflammation was included in the biopsy

Histopathology of another formalin-fixed biopsy specimen, taken from the target region 2 (Figure 1B,D), showed normally myelinated white matter with signs of slight microglia activation, but no evidence of inflammatory infiltrates or active demyelination (data

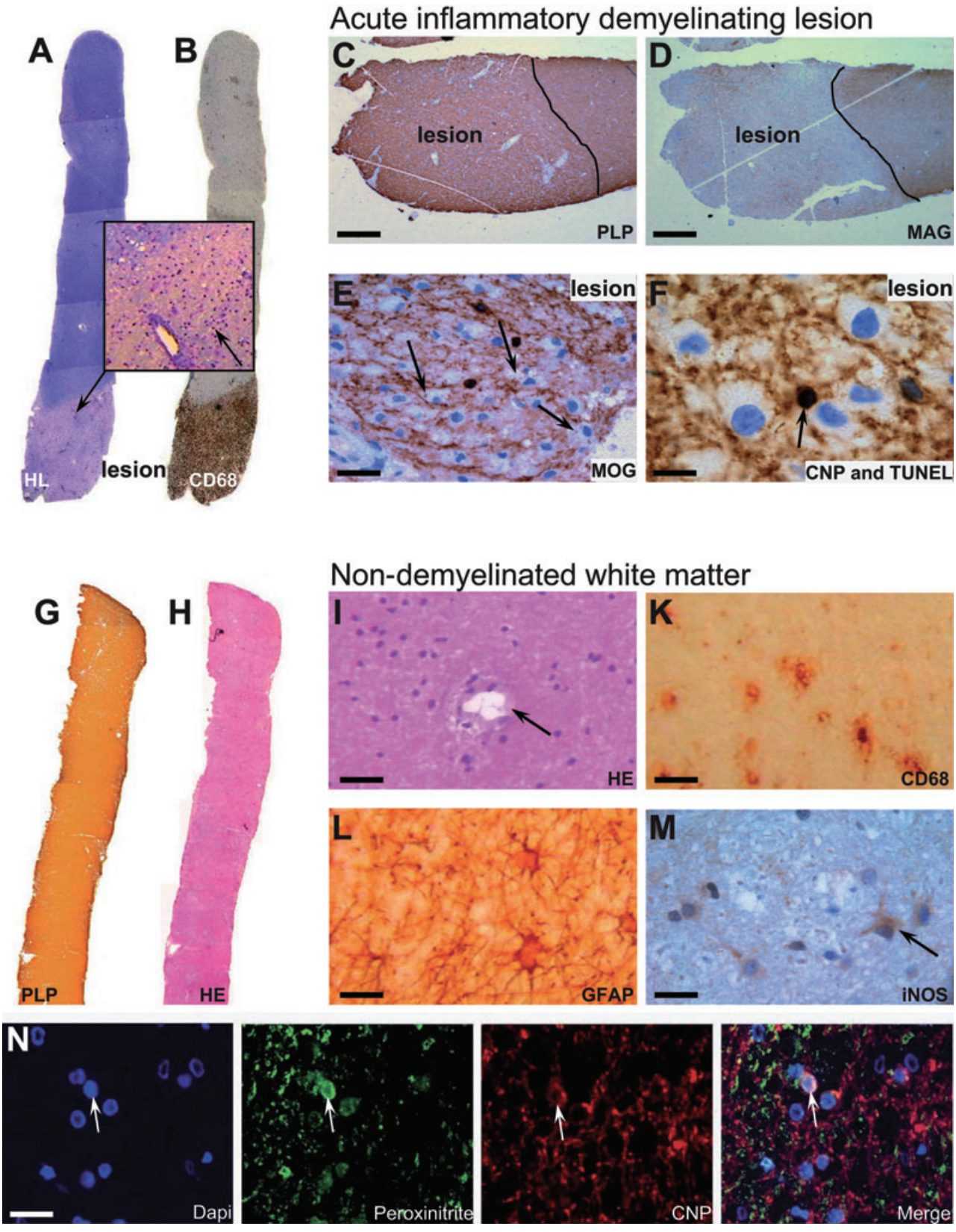

Figure 2. *Immunohistochemical analysis of lesion and non-demyelinated white matter tissue.* Immunopathological examination of paraffin-embedded biopsies containing lesion tissue (**A**–**F**) revealed a relatively sharp bordered lesion by Holmes/Luxol staining (**A**) with a dense infiltrate of CD68-positive macrophages (**B**). Inset of (**A**) shows dense infiltrating cells around a blood vessel (arrow). Staining for PLP in the acute lesion still appeared normal (**C**), whereas a specific absence of MAG was detected (**D**). Furthermore, MOG-positive myelin debris was detected within macrophages (**E**, arrows). TUNEL staining revealed apoptotic oligodendrocytes, co-stained by CNPase, within the lesion (**F**, arrow). Examination of the fresh-frozen biopsies used for RNA analysis did not show any signs of infiltrates or lesion formation (**G**–**M**). Staining by anti-PLP showed normal myelin (**G**), haematoxylin staining revealed normal cellularity (**H**) and blood vessels without infiltrating cells (**I**, arrow). However, a number of CD68-positive cells, histopathological microglia, were detected (**K**). Furthermore, activated astrocytes could be detected throughout the white matter (**L**). Staining for iNOS in non-demyelinated white matter distant to lesion revealed low expression levels in cells resembling microglia or astrocytes (**M,** arrow). Immunofluorescent colocalization for nitrotyrosine showed an accumulation in CNPase-positive oligodendrocytes (**N,** arrow). Bars: **C**, **D**: 100 μm; **E**: 30 μm; **F**: 25 μm; **I, K**: 50 μm; **L**, **M**, **N**: 25 μm.

not shown). One additional fixed biopsy specimen of target region 3 showed a small very focal, sharp bordered lesion alternating with histopathologically normal appearing tissue without any inflammatory infiltrates (data not shown). Analysis of all fresh frozen and formalin-fixed biopsy specimens revealed no signs of remyelination.

The two fresh snap-frozen biopsy tissue specimens, taken from target regions 2 and 3 (Figure 1B,D), revealed white matter with no signs of inflammation or demyelination (Figure 2G,H). This was evidenced by homogenous expression of PLP (Figure 2G) and other myelin proteins. Perivascular lymphocytes were absent (Figure 2I, arrow points to a blood vessel); however, a number of CD68-positive microglia were detected throughout the tissue (Figure 2K). In addition, activated astrocytes were evidenced by increased immunoreactivity for glial fibrillary acid protein (GFAP, Figure 2L). Signs of microglia and astrocyte activation may correspond to hypointense alterations observed on T1-weigthed MRI as well as hyperintense alterations on T2-weighted MRI (Figure 1A) (2, 8). Further, indication of early axonal alterations by the occurrence of dephosphorylated neurofilaments (SMI32) was detected (data not shown). However, no signs of axonal transection (bulbs) or loss were evident. These fresh-frozen white matter tissues, revealing no signs of demyelination or inflammation (Figure 2G–L)—although abnormal in MRI—were used for the qRT-PCR analysis.

Characterization of the non-demyelinated white matter reveals high levels of nNOS expression and nitric oxide-mediated damage of oligodendrocytes

To characterize earliest molecular changes in the non-demyelinated white matter, we performed quantitative RT-PCR for selected genes (Table 2). As NO is suggested to play an important role in MS pathogenesis and lesion formation, we investigated the expression pattern of the three NO-producing enzymes: nNOS, iNOS, and eNOS. The most striking result was the high expression level of nNOS in the non-demyelinated white matter of the index patient compared to the low nNOS expression levels in control as well as MS autopsies and also in control biopsy tissue (Table 2). We could also detect slightly elevated levels of the expression of iNOS and eNOS if compared with MS autopsies (Table 2). In contrast, iNOS expression in the index patient revealed a lower expression than the two control biopsy tissues from cases with malignant glioma, most likely representing microglial activation in the peritumoral normal white matter. Immunohistochemical analysis for iNOS revealed moderate expression in the non-demyelinated white matter of the index patient, most probably in microglia or astrocytes (Figure 2M, arrow). The low induction of iNOS expression was also evident by qRT-PCR (Table 2). In contrast, a high expression of iNOS was detected within the inflammatory lesion, where macrophages and activated microglia were strongly positive for iNOS (data not shown).

Staining of the non-demyelinated white matter with an anti-nitrotyrosine antibody revealed an accumulation of nitrotyrosine on myelin and oligodendrocytes distant from the actively demyelinating lesion (Figure 2N), pinpointing to a peroxynitrite-mediated damage to oligodendrocytes. However, apoptotic oligodendrocytes were only detected in the actively demyelinating lesion (Figure 2F).

Molecular analysis of the non-demyelinated white matter suggests early changes in oligodendrocytes

Because MS pattern III pathology was postulated to reflect an oligodendrogliopathy, we analyzed oligodendrocyte-specific genes involved in myelin maintenance. MOG and myelin basic protein displayed comparable expression levels in the index patient and control as well as MS autopsies and control biopsy tissues (Table 2). However, much higher expression levels of MAG and PLP were detected in the non-demyelinated white matter of the index patient. Compared with the expression levels of p.m. control tissue, an up-regulation of about four times was observed (Table 2). Furthermore, platelet-derived growth factor B, known to influence oligodendrocyte development (24), was tenfold up-regulated in the index patient in comparison to p.m. control and control biopsy tissues. Analysis of genes implicated in oligodendrocyte development and known to be expressed by oligodendrocyte precursor cells such as PDGFRα and EGR1/Krox24, revealed also increased expression levels in the index patient. However, a comparable expression level of PDGFRα was also detected in a young control autopsy (CLo9).

High expression of aquaporin 4 in non-demyelinated white matter

As the MRI analysis showed alterations in the white matter of the left hemisphere, and immunohistochemical staining for GFAP revealed activated astrocytes, we investigated astrocyte-specific genes such as GFAP, AQP4, as well as TAUT by qRT-PCR. Expression levels of AQP4 as well as GFAP were about five times higher than in the control cases (Table 2), further reflecting astrocyte activation and edema formation.

Table 2. Quantitative RT-PCR analysis of non-demyelinated white matter.

Genes	p.m. Controls	p.m. NAWM	Control biopsy tissues	Index patient n.d. WM	Fold Change vs. p.m. control median
Nitric oxide synthases					
nNOS	0.045 ± 0.043	0.044 ± 0.021	0.035 ± 0.018	**1.040**	***23.4***
iNOS	0.012 ± 0.007	0.012 ± 0.012	0.082 ± 0.017	**0.034**	***2.9***
eNOS	0.014 ± 0.012	0.020 ± 0.020	0.002 ± 0.001	**0.036**	***2.6***
Oligodendrocyte-related genes					
MOG	5.808 ± 3.380	6.272 ± 5.002	0.988 ± 0.331	**9.330**	1.6
MBP	573.6 ± 247.4	715.8 ± 664.5	32.58 ± 11.44	**522.4**	0.9
MAG	7.773 ± 1.365	7.888 ± 4.093	1.063 ± 0.095	**26.23**	***3.4***
PLP	9.678 ± 3.517	11.18 ± 6.970	5.675 ± 3.156	**42.01**	***4.3***
EGR1/Krox24	0.018 ± 0.015	0.044 ± 0.028	0.113 ± 0.112	**0.430**	24.6
PDGFB	0.039 ± 0.034	0.056 ± 0.026	0.048 ± 0.032	**0.408**	10.4
PDGFRA	0.147 ± 0.149	0.124 ± 0.094	0.099 ± 0.070	**0.393**	2.7
Astrocyte-related genes					
GFAP	68.35 ± 41.99	61.35 ± 36.53	5.135 ± 1.969	**333.6**	***4.9***
AQP4	5.393 ± 3.070	5.327 ± 3.143	2.533 ± 0.792	**24.47**	***4.6***
TAUT	0.798 ± 0.370	0.880 ± 0.168	0.077 ± 0.025	**1.485**	1.9
Neuroprotective genes					
HIF1A	0.616 ± 0.325	1.532 ± 0.564	0.212 ± 0.131	**0.873**	1.4
VEGFR	0.033 ± 0.021	0.072 ± 0.056	0.011 ± 0.005	**0.084**	2.6
HSP70.1	5.608 ± 4.298	8.738 ± 10.70	0.668 ± 0.433	**3.214**	0.6
HO-1	0.079 ± 0.042	0.118 ± 0.087	0.029 ± 0.007	**0.453**	***5.8***
Inflammation-related genes					
STAT4	0.015 ± 0.016	0.062 ± 0.083	0.394 ± 0.097	**0.034**	2.2
STAT6	0.045 ± 0.035	0.076 ± 0.026	0.039 ± 0.016	**0.904**	***20.3***
HLA-DRA	0.222 ± 0.389	0.368 ± 0.320	0.564 ± 0.189	**1.727**	***7.8***

Relative mRNA expression levels were calculated using the ribosomal gene L13A as a housekeeping gene. The table shows the average expression levels and the standard deviation of selected genes in p.m. control and p.m. NAWM tissue, as well as in disease control biopsies and in the non-demyelinated white matter tissue (n.d. WM). Fold changes show differences between the expression level of the index patient and the median of the expression levels of the p.m. control cases. Boxplot analysis for each gene is shown in the supplementary figure S1. Marked fold changes (bold, italic) show relevant up-regulated genes in the index patient compared with p.m. controls and control biopsies.
Abbreviations: p.m. = postmortem; n.d. = not detectable.

Induction of endogenous neuroprotective mechanisms in non-demyelinated white matter

In an earlier publication, we showed the up-regulation of endogenous neuroprotective genes in the normal-appearing white matter of MS autopsy cases (10, 30). Therefore, we selected specific protective genes for our analysis of the white matter of the present patient. In contrast to our previous study on p.m. brain tissue, heme oxygenase 1 (HO-1)—protective against oxidative stress and known to be expressed in oligodendrocytes, astrocytes and microglia (28)—showed a sixfold up-regulation in the white matter of the biopsy in comparison to p.m. control cases and an even higher up-regulation when compared to control biopsy tissue. On the other hand, the expression of HSP70.1, another protective protein which is induced mainly by heat shock and not by oxidative stress (9), was not changed. Also, in the case of HIF1α, a key regulator in hypoxic preconditioning and up-regulated in NAWM in chronic MS (10, 30), expression levels in the non-demyelinated white matter of the index patient were comparable to those from the p.m. control cases. If compared to the control biopsy tissue, slightly higher expression levels of HIF-1α could be observed in the non-demyelinated white matter of the index patient. Nevertheless, under acute hypoxic conditions, activation of HIF1α is fulfilled by stabilizing the protein rather than mRNA up-regulation (7). Indeed, the up-regulation of VEGFR, a downstream gene of HIF1α, indicates possible HIF1α activation (23). Altogether, the up-regulation of HO-1 as well as VEGFR suggests an activation of protective mechanisms against oxidative stress in the non-demyelinated white matter in pattern III MS.

Up-regulation of anti- as well as pro-inflammatory genes in non-demyelinated white matter

Autoimmunity plays a major role in the pathology of MS. We and others have recently suggested an involvement of innate immune mechanisms in MS (3, 30). We thus examined the expression of selected genes involved in innate inflammatory mechanisms, which we had already studied in p.m. NAWM (Table 2) (30). A major finding was the 20-fold increase in STAT6, an anti-inflammatory transcription factor which we found to be expressed by oligodendrocytes in the MS NAWM (30). The expression level of STAT4, a major pro-inflammatory transcription factor, in the index patient was comparable to p.m. control tissues, although almost all of them showed a lower STAT4 expression. In the control biopsy tissues, STAT4 was highly elevated in comparison to the index patient as well as the p.m. control and MS NAWM cases. In

contrast, HLA-DRA showed a strong up-regulation in the index patient compared to the control biopsy tissues and the p.m. control and p.m. MS NAWM cases.

DISCUSSION

This study reports earliest molecular changes in non-demyelinated white matter during the first manifestation of an actively demyelinating pattern III MS case. Although all white matter tissue specimens of the index patient were taken from brain areas showing abnormal MRI signals, histopathological examination of the specimens used for RNA extraction revealed white matter without any signs of inflammation, demyelination, or remyelination. The p.m. control and MS NAWM subcortical white matter tissues, as well as white matter tissue form control biopsy tissue were used in this study and were analyzed for confounding pathology such as signs of inflammation, demyelination, microglia activation, and gliosis.

As a major finding, we show that nNOS is strongly up-regulated in non-demyelinated white matter during a very early, acute phase of MS. As nNOS gene expression levels of two control biopsy tissues as well as a young control autopsy case (CLo9, Table 1) was comparable to that of p.m. control cases, this up-regulation most likely represents a disease-specific mechanism and not an age-related artifact. Recent data showed that nNOS plays a key role in mediating CNS demyelination in a toxin-induced demyelinating animal model (13). The presence of toxic NO is further supported by the finding of nitrotyrosine-positive oligodendrocytes, suggesting early NO-mediated oligodendrocyte damage. Thus, up-regulation of nNOS in the non-demyelinated white matter may reflect early brain intrinsic changes in pattern III MS, possibly impairing oligodendrocyte homeostasis and myelin sheath maintenance, and by that maybe facilitating demyelination. Although nNOS was highly expressed, overt apoptotic oligodendrocytes were not detectable in the non-demyelinated white matter, suggesting sublethal damage to oligodendrocytes not reaching the apoptotic threshold. Alternatively, oligodendrocyte death might be prevented by simultaneously induced protective mechanisms (29). This is consistent with our observation of the up-regulation of heme oxygenase HO-1, which is known to be protective against NO-mediated damage (19) as well as by inhibiting leucocyte accumulation in the CNS (6). Ongoing alterations in oligodendrocytes were further indicated by the up-regulation of PLP and MAG mRNA, which could reflect some stress-related compensatory mechanisms in oligodendrocytes, or alternatively might be specific for pattern III MS. The up-regulation of particular genes in oligodendrocytes, such as STAT6, MAG, or PLP, might further strengthen the assumption of ongoing brain intrinsic events. Whether these alterations distant from demyelinating lesion may facilitate or impede lesion formation cannot be said. However, the consideration that these changes could possibly contribute to the lesion formation is supported by earlier studies suggesting that early oligodendrocyte injury might be the initial event in MS (18, 20, 21). Additionally, Barnett and Prineas suggested widespread oligodendrocyte damage and apoptosis as one of the earliest change in lesion formation (1), which are comparable to our observation. In the study of Barnett and Prineas, apoptotic oligodendrocytes were found in lesions as well as periplaque areas, whereas in contrast we did not find apoptotic oligodendrocytes in the non-demyelinated white matter. Therefore, one may speculate that the non-demyelinated white matter examined in our study might even be in an earlier stage, or at a larger distance from the active lesion than that examined by Barnett and Prineas. This is further supported by our finding of nitrotyrosine-positive oligodendrocytes in the non-demyelinated white matter. Whether this is specific for a subset of MS patients (pattern III lesions) or a general phenomenon in MS pathology needs to be further elucidated.

Another explanation for nNOS expression in the non-demyelinated white matter might be activated astrocytes, as these cells were shown to increase expression of nNOS under pathological conditions (4, 12). Activation of astrocytes is also evident by the up-regulation of GFAP, AQP4, and TAUT. Nevertheless, the inducible isoform of NOS (iNOS) was only moderately up-regulated, additionally supporting the concept that rather brain intrinsic changes than primary immune reactions are causative for the observed differential gene expression in the non-demyelinated white matter. Another finding was a strong up-regulation of STAT6 whereas STAT4 expression was only slightly elevated. This is in-line with our previous report in which we found an up-regulation of STAT6 and its downstream genes in p.m. MS cases (30). In EAE, it has been shown that STAT6 deficient mice show a more severe clinical course, whereas STAT4-deficient mice are resistant to the induction of MOG-induced EAE (5). In contrast, in a TMEV model with a very prolonged incubation period, the lack of STAT4 led to a severe demyelination, whereas in STAT6-deficient mice, demyelination was minimal (22). The question, whether in MS this strong induction of STAT6 in contrast to the slight expression of STAT4 is beneficial or detrimental has to be further elucidated.

Although abnormalities in a large area of the left hemisphere have been detected on T1- and T2-weighted MRI, only a small part of the biopsy specimens contained areas of inflammatory demyelination. We conclude from our study that even in large T1 and T2 abnormalities, there remains non-demyelinated white matter without overt signs of inflammation. This is in agreement with a study from Fisher *et al* 2007 showing that T1 and T2 MRI abnormalities do not necessarily imply demyelination and lesion formation (8). Still, our data indicate activated microglia, astrogliosis, and edema formation, which may not yet reach a pathological level leading to tissue destruction, but disclose intrinsic molecular alterations.

Taken together, our study suggests that earliest molecular changes are present in the non-demyelinated white matter distant from an active inflammatory demyelinating lesion. The changes in the non-demyelinated white matter might be crucial for lesion initiation and the further development of the disease, determining lesion progression or limitation. Therapeutical modulation of these alterations in the white matter might be an important target for the prevention of tissue damage in MS.

ACKNOWLEDGMENTS

We thank Prof. Dr. Ph. Lyrer, Prof. Dr. L. Kappos, J. Hoepfl (Department of Neurology, University Hospital Basel), and Prof. Dr. C. Buitrago (Hospital Zofingen, Switzerland) for helpful discussions. We thank Dr. Tanja Kuhlmann (Neuropathology, Georg-August-University Göttingen) and B. Erne (Neurobiology, University Hospital Basel) for technical assistance. Stereotactic brain biopsy was performed by Dr. M. Wasner (Neurosurgery, University Hospital Basel). We thank Prof. Dr. R. Reynolds and the UK

MS Tissue Bank at Imperial College (London) for the provision of tissue for this study. This work was supported by the National Multiple Sclerosis Societies of Switzerland, France (ARSEP), United Kingdom, and United States of America, and by the Gemeinnützige Hertie-Stiftung. CS is supported by the Medical Faculty of Goettingen (junior research group).

REFERENCES

1. Barnett MH, Prineas JW (2004) Relapsing and remitting multiple sclerosis: pathology of the newly forming lesion. *Ann Neurol* **55**:458–468.
2. Bruck W, Bitsch A, Kolenda H, Bruck Y, Stiefel M, Lassmann H (1997) Inflammatory central nervous system demyelination: correlation of magnetic resonance imaging findings with lesion pathology. *Ann Neurol* **42**:783–793.
3. Cannella B, Raine CS (2004) Multiple sclerosis: cytokine receptors on oligodendrocytes predict innate regulation. *Ann Neurol* **55**:46–57.
4. Catania MV, Aronica E, Yankaya B, Troost D (2001) Increased expression of neuronal nitric oxide synthase spliced variants in reactive astrocytes of amyotrophic lateral sclerosis human spinal cord. *J Neurosci* **21**:RC148.
5. Chitnis T, Najafian N, Benou C, Salama AD, Grusby MJ, Sayegh MH, Khoury SJ (2001) Effect of targeted disruption of STAT4 and STAT6 on the induction of experimental autoimmune encephalomyelitis. *J Clin Invest* **108**:739–747.
6. Chora AA, Fontoura P, Cunha A, Pais TF, Cardoso S, Ho PP *et al* (2007) Heme oxygenase-1 and carbon monoxide suppress autoimmune neuroinflammation. *J Clin Invest* **117**:438–447.
7. Dery MA, Michaud MD, Richard DE (2005) Hypoxia-inducible factor 1: regulation by hypoxic and non-hypoxic activators. *Int J Biochem Cell Biol* **37**:535–540.
8. Fisher E, Chang A, Fox RJ, Tkach JA, Svarovsky T, Nakamura K *et al* (2007) Imaging correlates of axonal swelling in chronic multiple sclerosis brains. *Ann Neurol* **62**:219–228.
9. Goldbaum O, Richter-Landsberg C (2001) Stress proteins in oligodendrocytes: differential effects of heat shock and oxidative stress. *J Neurochem* **78**:1233–1242.
10. Graumann U, Reynolds R, Steck AJ, Schaeren-Wiemers N (2003) Molecular changes in normal appearing white matter in multiple sclerosis are characteristic of neuroprotective mechanisms against hypoxic insult. *Brain Pathol* **13**:554–573.
11. Jack C, Antel J, Bruck W, Kuhlmann T (2007) Contrasting potential of nitric oxide and peroxynitrite to mediate oligodendrocyte injury in multiple sclerosis. *Glia* **55**:926–934.
12. Kim S, Moon C, Wie MB, Kim H, Tanuma N, Matsumoto Y, Shin T (2000) Enhanced expression of constitutive and inducible forms of nitric oxide synthase in autoimmune encephalomyelitis. *J Vet Sci* **1**:11–17.
13. Linares D, Taconis M, Mana P, Correcha M, Fordham S, Staykova M, Willenborg DO (2006) Neuronal nitric oxide synthase plays a key role in CNS demyelination. *J Neurosci* **26**:12672–12681.
14. Lucchinetti C, Bruck W, Parisi J, Scheithauer B, Rodriguez M, Lassmann H (2000) Heterogeneity of multiple sclerosis lesions: implications for the pathogenesis of demyelination. *Ann Neurol* **47**:707–717.
15. Lucchinetti CF, Brueck W, Rodriguez M, Lassmann H (1998) Multiple sclerosis: lessons from neuropathology. *Semin Neurol* **18**:337–349.
16. McDonald WI, Compston A, Edan G, Goodkin D, Hartung HP, Lublin FD *et al* (2001) Recommended diagnostic criteria for multiple sclerosis: guidelines from the International Panel on the Diagnosis of Multiple Sclerosis. *Ann Neurol* **50**:121–127.
17. Poser CM (2006) Revisions to the 2001 McDonald diagnostic criteria. *Ann Neurol* **59**:727–728.
18. Prineas JW, Connell F (1978) The fine structure of chronically active multiple sclerosis plaques. *Neurology* **28**:68–75.
19. Reiter TA, Demple B (2005) Carbon monoxide mediates protection against nitric oxide toxicity in HeLa cells. *Free Radic Biol Med* **39**:1075–1088.
20. Rodriguez M, Scheithauer B (1994) Ultrastructure of multiple sclerosis. *Ultrastruct Pathol* **18**:3–13.
21. Rodriguez M, Scheithauer BW, Forbes G, Kelly PJ (1993) Oligodendrocyte injury is an early event in lesions of multiple sclerosis. *Mayo Clin Proc* **68**:627–636.
22. Rodriguez M, Zoecklein L, Gamez JD, Pavelko KD, Papke LM, Nakane S *et al* (2006) STAT4- and STAT6-signaling molecules in a murine model of multiple sclerosis. *FASEB J* **20**:343–345.
23. Semenza GL (2001) Hypoxia-inducible factor 1: oxygen homeostasis and disease pathophysiology. *Trends Mol Med* **7**:345–350.
24. Silberstein FC, De Simone R, Levi G, Aloisi F (1996) Cytokine-regulated expression of platelet-derived growth factor gene and protein in cultured human astrocytes. *J Neurochem* **66**:1409–1417.
25. Smith KJ, Lassmann H (2002) The role of nitric oxide in multiple sclerosis. *Lancet Neurol* **1**:232–241.
26. Stadelmann C, Bruck W, Bancher C, Jellinger K, Lassmann H (1998) Alzheimer disease: DNA fragmentation indicates increased neuronal vulnerability, but not apoptosis. *J Neuropathol Exp Neurol* **57**:456–464.
27. Stadelmann C, Ludwin S, Tabira T, Guseo A, Lucchinetti CF, Leel-Ossy L, *et al* (2005) Tissue preconditioning may explain concentric lesions in Balo's type of multiple sclerosis. *Brain* **128**:979–987.
28. Stahnke T, Stadelmann C, Netzler A, Bruck W, Richter-Landsberg C (2007) Differential upregulation of heme oxygenase-1 (HSP32) in glial cells after oxidative stress and in demyelinating disorders. *J Mol Neurosci* **32**:25–37.
29. Zeis T, Schaeren-Wiemers N (2008) Lame ducks or fierce creatures?—the role of oligodendrocytes in multiple sclerosis. *J Mol Neurosci* **35**:91–100.
30. Zeis T, Graumann U, Reynolds R, Schaeren-Wiemers N (2008) Normal-appearing white matter in multiple sclerosis is in a subtle balance between inflammation and neuroprotection. *Brain* **131**:288–303.

SUPPORTING INFORMATION

Additional Supporting Information may be found in the online version of this article:

Figure S1. Boxplot analysis of selected differentially expressed genes analyzed by qRT-PCR. mRNA expression levels were normalized to the ribosomal house keeping gene L13A. Boxplots show differential gene expression of selected genes in p.m. control and p.m. NAWM tissue, as well as in the non-demyelinated white matter tissue of the index patient (n.d.WM) and in disease control biopsies. qRT-PCR was performed for nNOS (A), iNOS (B), eNOS (C), MOG (D), MBP (E), MAG (F), PLP (G), EGR1 / Krox24 (H), PDGFRalpha (I), GFAP (K), Aqp4 (L), TAUT (M), PDGFB (N), HIF-1alpha (O), VEGFR1 (P), HSP70.1 (Q), HO-1 (R), STAT4 (S), STAT6 (T) and HLA-DRalpha (U).

Please note: Wiley-Blackwell are not responsible for the content or functionality of any supporting materials supplied by the authors. Any queries (other than missing material) should be directed to the corresponding author for the article.